LA-5865

c. 2

UC-34
Reporting Date: January 1975
Issued: April 1975

# Nonsteady-State Detonations in One-Dimensional Plane, Diverging, and Converging Geometries


by

Charles L. Mader
B. G. Craig





los alamos
scientific laboratory
of the University of California
LOS ALAMOS, NEW MEXICO 87544

An Affirmative Action/Equal Opportunity Employer

UNITED STATES
ENERGY RESEARCH AND DEVELOPMENT ADMINISTRATION
CONTRACT W-7405-ENG. 36

Printed in the United States of America. Available from
National Technical Information Service
U S Department of Commerce
5285 Port Royal Road
Springfield, VA 22151
Price: Printed Copy $4.00 Microfiche $2.25

NONSTEADY-STATE DETONATIONS IN ONE-DIMENSIONAL PLANE,

DIVERGING, AND CONVERGING GEOMETRIES

by

Charles L. Mader and B. G. Craig

ABSTRACT

Experimental evidence is described demonstrating that detonation waves in one-dimensional plane geometry are not steady state. The effective Chapman-Jouguet pressure is observed to increase as the detonation wave runs. A detonation build-up model was developed that can be used with numerical hydrodynamic computer programs to reproduce the observed behavior of nonsteady-state detonations in plane geometry.

Using the detonation build-up model, the one-dimensional flow of spherically and cylindrically diverging detonation waves can be closely approximated as evidenced by the agreement with experimental data. The effect of detonation build-up in diverging geometry is masked by the larger divergence effect.

The one-dimensional flow of converging detonations can be closely approximated using the build-up model. The convergence effect on detonations can be described by appropriate scaling of the state parameters.



## I. INTRODUCTION

Most of the results in this report were previously described by Mader in 1968. Until November 1974, the concept of detonation build-up was classified. For more than 6 yr the results described in this report have been applied successfully to many engineering problems. Several critical experiments to test the detonation build-up concept have been performed since its initial description became available to the classified technical community. This report contains the declassified portions of the earlier work and some of the newer results that have not been previously published.

The first observation of build-up of detonation was for the explosive, PBX-9404. Build-up of detonation has also been observed for the explosives, Composition B and TNT.

In 1965, Craig[1] first discovered the nature of the nonsteady behavior of explosives. He studied the interaction of the explosive 9404 in one-dimensional plane geometry at four charge lengths with Dural, magnesium, and Plexiglas plates. If the 9404 has steady-state behavior, the experimental data should have scaled as a function of plate vs explosive thickness. The data did not scale and the data clearly indicate that the effective Chapman-Jouguet (C-J) pressure ($P_{ECJ}$) for underinitiated detonating 9404 increases, or builds up as the detonation wave runs.

The result was not unexpected, because at about the same time, Davis et al.[2] had shown from other experimental studies that the steady-state C-J theory did not accurately describe the behavior of real explosives. The exact nature of the nonsteady-state behavior shown by Craig's data[1] (a change of 25% in $P_{ECJ}$ with less than 1% in detonation velocity) was a surprise to most detonation scientists; however, it permitted one to understand why thin layers of explosives behaved so differently than expected from the simple calculations calibrated with data from thicker explosive charges.

The physical and chemical processes that cause the nonsteady-state behavior of explosives are still unknown. Mader[3] has shown that the solution of the Navier-Stokes equations of fluid dynamics, using Arrhenius chemical reaction and accurate equations of state for condensed explosives, results in detonations that exhibit unstable periodic behavior. The steady-state Chapman-Jouguet theory of the detonation process cannot properly describe the behavior of real explosives that exhibit unstable periodic behavior. Mader's calculations give no hint of the nature of the actual behavior that is to be expected and may have no physical reality because the real chemical reactions are more complicated than is assumed by the calculations. Real explosives,[4] that have solid carbon as a detonation product, exhibit behavior that is not adequately described without the inclusion of some time-dependent phenomenon, such as diffusion-controlled carbon deposition or some other kinetic behavior of the detonation products. A time-dependent carbon deposition is the only process we have considered that could account for the large energy deficits required by our model. The obvious test of such a suggestion, that of studying the build-up behavior of an oxygen-rich explosive, has not been performed.

Although we have clues indicating the processes that result in failure of the steady-state detonation model, they are currently of little value to the numerical engineer who wishes to treat an explosive as realistically as practicable. He would like a description of the explosive behavior that would work in divergent and convergent geometry as well as plane geometry. We shall limit our discussion to one-dimensional flow, not because of a lack of interest in two- and three-dimensional flow, but because the multidimensional problem appears extremely complicated, as evidenced by studies[5] of simple two-dimensional detonations.

## II. THE BUILD-UP MODEL

This report describes the numerical results obtained modeling various experimental studies with the build-up model. We assume that a real nonsteady-state detonation can be adequately approximated by a series of steady-state detonations with instantaneous reaction whose "effective C-J pressures" vary with the distance of run. This empirical model depends completely upon experimental data for its calibration. If one changes the magnitude or duration of the initiating pulse or changes the explosive from one for which experimental data are available, new experimental data must be generated and the model calibrated for the new system.

It is important to understand that this discussion is about the build-up of the effective C-J pressure of detonating 9404 initiated at pressures less than infinite-medium effective C-J pressure, but greater than that pressure required for prompt initiation (~100 kbar for most explosives). This is not to be confused with the build-up to detonation, characteristic of the process of shock initiation of heterogeneous explosives initiated by a shock wave of a few tens of kilobars.[6]

Because the nonsteady-state detonation process requires new concepts, some appropriate definitions are given below.

Build-Up TO Detonation - Characteristic of the process of shock initiation of heterogeneous explosives initiated by a shock wave of a few tens of kilobars.

Build-Up OF Detonation - The change of the effective C-J pressure of a detonating explosive initiated at pressures less than infinite-medium effective C-J pressures, but greater than that required for relatively prompt initiation.

The Build-Up Model - An empirical model for engineering purposes that depends on experimental data for calibration. The model assumes that a real nonsteady-state detonation can be adequately approximated by a series of steady-state detonations with instantaneous reaction and constant detonation velocity whose effective C-J pressures vary with the distance of run for a particular initiation system.

Effective C-J Pressure - The maximum pressure of a completely decomposed explosive in a steady-state detonation, used to approximate the nonsteady-state flow associated with a particular distance of run and initiating system.

Infinite-Medium Effective C-J Pressure - The actual steady-state C-J detonation pressure for an explosive. In practical plane wave systems, it can only be achieved if the explosive is initially overdriven.

Peak Detonation Pressure - The largest pressure obtained in diverging or converging flow after some distance of travel, using an equation of state with an effective C-J pressure that is characteristic of some distance of run in slab geometry.

## III. THE NUMERICAL METHODS

We used the SIN code[7] to compute most of the one-dimensional problems described in this report. For a few problems, the characteristic code RICSHAW,[8] as revised by Rivard, was used to check the results obtained with SIN.

We studied the methods of burning the explosive to determine if the numerical results were independent of the burn technique. The gamma-law Taylor wave burn technique for slabs, the Arrhenius rate law, and the C-J volume burn technique are described in Ref. 7. The sharp-shock burn technique is described in Ref. 6. Another method in common use is the programmed burn, which assumes that the time to burn an explosive cell can be predetermined from the detonation velocity. Any of the methods is satisfactory for plane geometry, but the gamma-law Taylor wave method is faster and requires fewer cells in the numerical calculation. For divergent geometry, the Arrhenius rate law gives the best results; however, the C-J volume burn technique can be used if, in addition to the usual prescription,[7] the cell burn is completed when expansion of the cell begins. The sharp-shock burn technique of SIN or RICSHAW cannot be used in divergent geometry. In convergent geometry, the C-J volume burn, Arrhenius rate law, or sharp-shock burn of SIN or RICSHAW can be used. The programmed burn technique can be used if one can predetermine how the detonation velocity changes with convergence. In Sec. IX, we show how this is possible to a good first approximation, and therefore the programmed burn technique can be used in convergent geometry.

Most of the plane calculations used 400 cells or space increments in the metal and 250 cells in the explosive. Most of the calculations of spherically diverging detonations were performed with 600 cells in the explosive and 300 cells in the metal. Most of the calculations of spherically converging detonations used 800 cells in the explosive.

The equation of state used was the HOM equation of state.[7] The Hugoniot of the aluminum was described using experimentally determined linear shock velocity $U_s$ and particle velocity $U_p$ curves, expressed as $U_s = C + SU_p$. The constants used, which are identical to those in Ref. 7, are given below.

| Metal | $\rho_o$ | C | S | $\gamma$ | $\alpha$ | $C_V$ |
|---|---|---|---|---|---|---|
| Al | 2.785 | 0.535 | 1.35 | 1.7 | $2.4 \times 10^{-5}$ | 0.22 |

Generally, the PIC form[7] of the viscosity was used with a constant of 2.0.

The gamma-law equation of state for a steady-state detonation is described below for the convenience of the reader.

$$P_{CJ} V_{CJ}^{\gamma} = C \quad ,$$

$$V_{CJ} = \frac{\gamma V_o}{\gamma + 1} \quad ,$$

$$\ell n \, P_i = \ell n \, C - \gamma \, \ell n \, V \quad ,$$

$$I_i = \frac{PV}{\gamma - 1} - \frac{P_{CJ} V_{CJ}}{\gamma - 1} + \frac{P_{CJ}}{2} (V_o - V_{CJ}) \quad .$$

Given the initial density, $\rho_o$, detonation velocity, D, and $P_{CJ} = \frac{\rho_o D^2}{\gamma + 1}$, the isentrope of the detonation products is defined for any given $P_{CJ}$, $\gamma$, or $V_{CJ}$. One calculates off the isentrope by using the constant beta equation of state

$$P = \frac{1}{(\beta V)} (I - I_i) + P_i \quad ,$$

where

$$\beta = \frac{1 + \alpha}{\gamma} \quad \text{and} \quad \alpha = \left[ \frac{(\gamma + 1)}{\left(1 + \frac{d(\ell n \, D)}{d(\ell n \, \rho)}\right)} - 2 \right]^{-1} \quad .$$

A value of 0.66 was used for the $d(\ell n \, D)/d(\ell n \, \rho)$ of

9404, and β varied from 1.30 at $P_{ECJ}$ = 0.365 Mbar to 0.607 at $P_{ECJ}$ = 0.306 Mbar.

Throughout this report the "gamma-law equation of state" means that the gamma-law equation is used to describe the isentrope through the C-J point and the constant beta equation is used to calculate off the isentrope. The "BKW equation of state" means that the Becker-Kistiakowsky-Wilson[4] equation of state is used to describe the isentrope through the C-J point and a variable beta equation of state is used to calculate off the isentrope, with beta a function of volume as defined by the BKW equation of state.

## IV. BUILD-UP OF 9404 IN PLANE GEOMETRY

Craig's experimental data show that the effective C-J pressure of underinitiated, detonating 9404 increases or builds up as the detonation wave runs. Craig found that the effective C-J pressure increases with distance as shown in Fig. 1 for 9404 initiated with a Baratol plane wave lens. Effective C-J pressures were obtained using Dural, magnesium, and Plexiglas plates that were identical within experimental error for the same distance of run. The experimental data used in Fig. 1 are given in Table I. Craig also observed that the detonation wave velocity remains within 100 m/s of 8800 m/s for all the systems studied. Assuming that a real nonsteady-state detonation can be approximated by a series of steady-state detonations whose effective C-J pressures vary with the distance of run, we can use

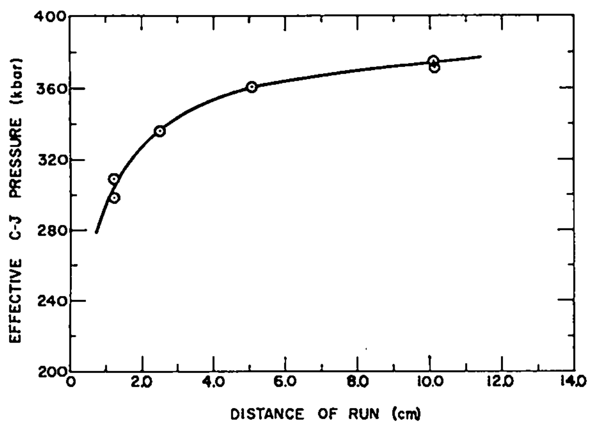


Fig. 1. Craig's experimental effective C-J pressures of 9404 vs distance of run for Baratol plane wave initiation of 9404 slabs.

$$\gamma = \left(\rho_o D^2/P_{ECJ}\right) - 1 \quad ,$$

(where $\rho_o$, the initial density, is 1.844 g/cm$^3$, D, the detonation velocity, 0.88 cm/μs, and $P_{ECJ}$ is the effective C-J pressure in Mbar) to calculate gamma as a function of distance of run as shown in Fig. 2. This may be described by the equation called the "build-up equation"

$$\gamma = 2.68 + 1.39/(\text{distance of run in cm})$$

or

$$\gamma = 2.68 + 1.58/(\text{time of run in μs}) \quad .$$

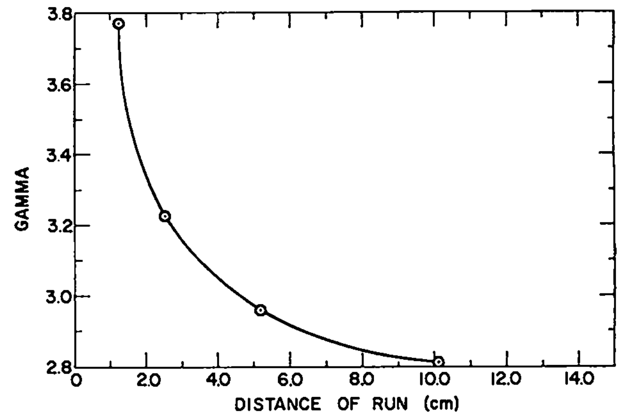


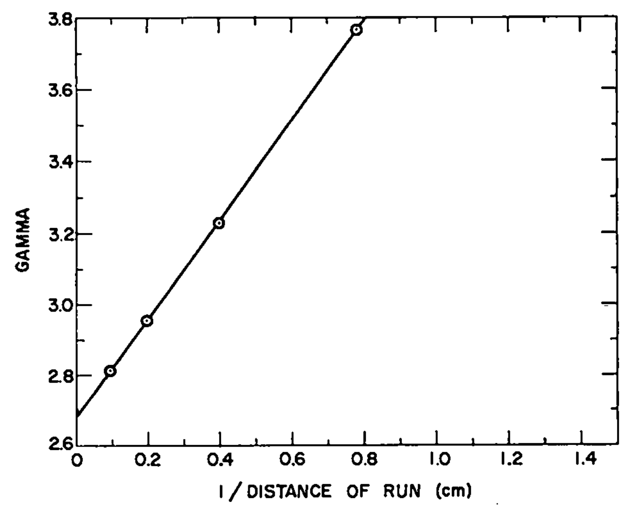


Fig. 2. Gamma-law equation of state gamma calculated using Craig's experimental effective C-J pressures of 9404 vs distance of run and vs the reciprocal of the distance of run.

TABLE I

9404 EXPERIMENTAL DATA

| Charge Length (cm) | Charge Diameter (cm) | Plate Material | Plate Thickness (mm) | Free-Surface Velocity (mm/μs) | Initiation (Diameter Baratol lens - cm) | Length/ Diameter Ratio | $P_{ECJ}$ (kbar) |
|---|---|---|---|---|---|---|---|
| 1.27 | 10.16 | 2024 ST Dural | 3.2 | 3.12 | 10.16 | 0.125 | 303 |
| | | | 4.5 | 3.03 | | | |
| | | | 6.4 | 2.92 | | | |
| | | | 12.7 | 2.57 | | | |
| 1.27 | 30.48 | 2024 ST Dural | 3.27 | 3.20 | 30.48 | 0.0416 | 312 |
| | | | 4.55 | 3.13 | | | |
| 1.27 | 10.16 | Magnesium | 3.34 | 4.18 | 10.16 | 0.125 | 306 |
| | | | 3.72 | 4.14 | | | |
| | | | 5.00 | 4.10 | | | |
| | | | 7.83 | 3.95 | | | |
| 2.54 | 20.32 | 2024 ST Dural | 2.20 | 3.45 | 20.32 | 0.125 | 335 |
| | | | 2.50 | 3.45 | | | |
| | | | 4.50 | 3.39 | | | |
| | | | 6.35 | 3.33 | | | |
| | | | 12.70 | 3.075 | | | |
| | | | 25.40 | 2.675 | | | |
| 5.08 | 30.48 | 2024 ST Dural | 2.81 | 3.67 | 30.48 | 0.167 | 358 |
| | | | 4.59 | 3.61 | | | |
| | | | 12.17 | 3.47 | | | |
| | | | 21.0 | 3.27 | | | |
| 10.16 | 30.48 | 2024 ST Dural | 3.13 | 3.90 | 30.48 | 0.333 | 375 |
| | | | 25.4 | 3.45[a] | | | |
| | | | 50.9 | 3.02[a] | | | |
| 10.16 | 30.48 | Plexiglas | 6.0 | 6.00 | 30.48 | 0.333 | 372 |
| | | | 12.0 | 5.65[a] | | | |
| | | | 24.5 | 5.34[a] | | | |
| | | | 51.0 | 4.66[a] | | | |

[a]Believed to be two-dimensional.

The fit was used down to 0.8 μs (0.704 cm); then, the gamma was kept constant at 4.655 ($P_{ECJ}$ = 0.252 Mbar) for shorter times and distances of run. This arbitrary limit was imposed to prevent the fit from giving unreasonable results for short times and distances of run. Although this permits us to obtain good estimates of the effective C-J pressure, we still have the problem of how to best describe the

Taylor wave. We ran calculations for the experimental geometries studied by Craig, assuming that the entire explosive burned with the constant gamma for the total distance of run, and also with the gamma varying through the flow according to the build-up equation described above. For the latter case, the gamma of each cell was held constant at its value when the detonation wave first passed through it. The Taylor waves are shown in Figs. 3 and 4 and their effect on the Dural plate motion is shown in Fig. 5. To a very good first approximation, we can use a constant gamma for the total distance of run to describe the Taylor wave.

It is interesting to note that from 4-10 cm of run, the effective C-J pressure varies only from 350-375 kbar. Most plane wave experimental studies are in this range of run. The usual effective C-J pressure stated for 9404 is 365 kbar. The actual infinite-medium effective C-J pressure of 9404 is approximately 400 kbar. The 365-kbar value was determined by Deal some 15 yr ago using a charge geometry that was 14.2-cm-long and 14.2-cm diameter. We believe this system is two-dimensional. The effect of the side rarefactions is shown in Fig. 6, where the experimental free-surface velocities are

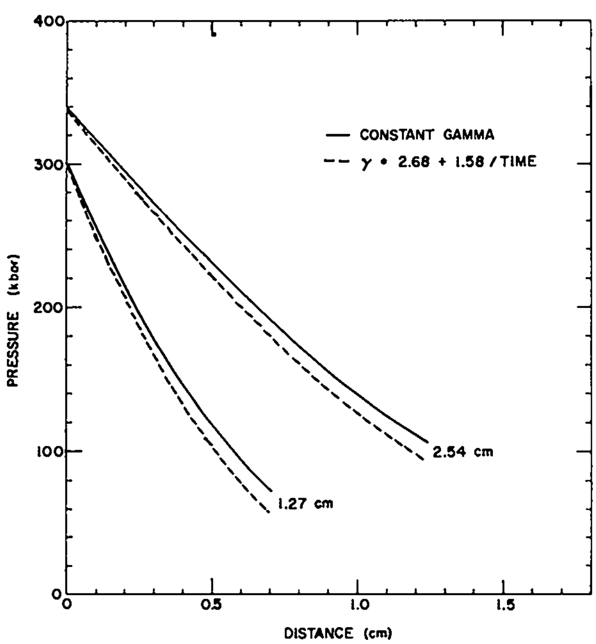


Fig. 3. Calculated Taylor waves for 1.27 and 2.54 cm of 9404 with constant gammas of 3.77 and 3.227, respectively, and with a variable gamma.

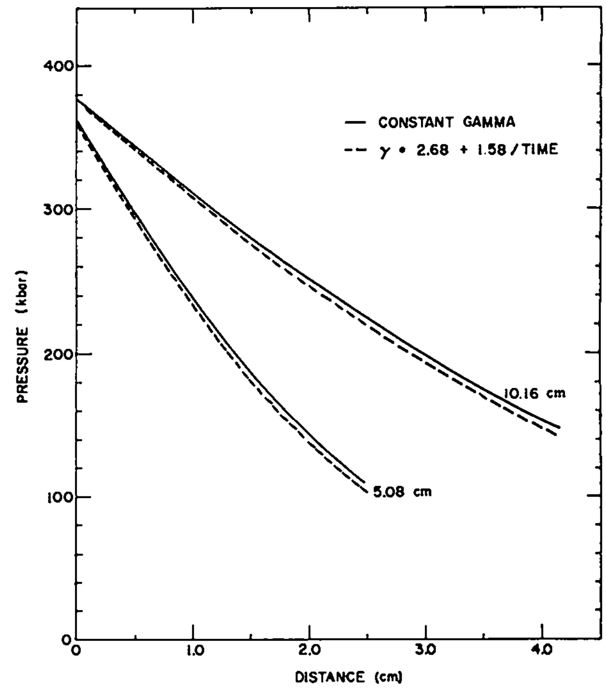


Fig. 4. Calculated Taylor waves for 5.08 and 10.16 cm of 9404 with a constant gamma of 2.9536 and 2.817, respectively, and with a variable gamma.

markedly lower than the calculated velocities as the metal is affected by more of the Taylor wave. It is thus a matter of luck that the two-dimensional effects lowered the extrapolated pressure into the range where most plane wave experiments are performed. This is why the BKW equation of state calibrations,[4] using Deal's effective C-J pressures, worked so well in describing most plane wave experimental data. Our build-up model will not work for slab systems whose length-to-diameter ratio is greater than 0.25 and which are not supported by a plane wave. The reason such a small value for the length-to-diameter ratio is chosen is that most plane wave systems are sufficiently plane and uniform only over the inside half or less of their diameter, so only the inner half of the explosive charge is properly supported. The small length-to-diameter ratio also is chosen to eliminate the effect of side rarefactions while the shock travels through the metal plate. This concept is not accepted by Bdzil and Davis[9] as is discussed in Sec. VII.

The effect of changing the magnitude of the initiating pulse can be estimated by shifting the

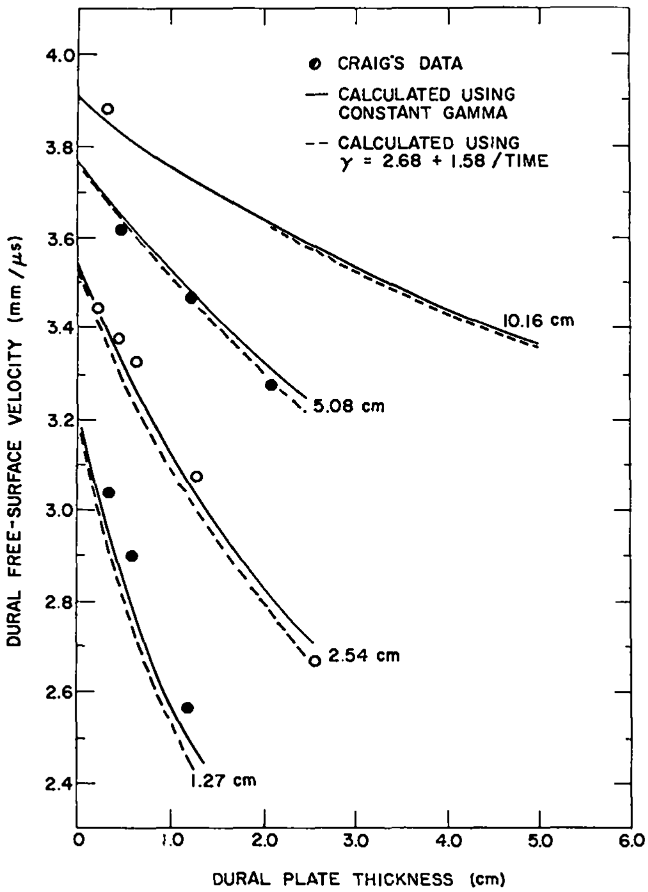


Fig. 5. Dural free-surface velocities vs Dural plate thickness for 1.27, 2.54, 5.08, and 10.16 cm of 9404. Curves show Craig's data and the calculated results obtained for constant gamma Taylor waves (3.77, 3.227, 2.9536, and 2.817, respectively) and $\gamma = 2.68 + 1.58/\text{Time}$ Taylor wave.

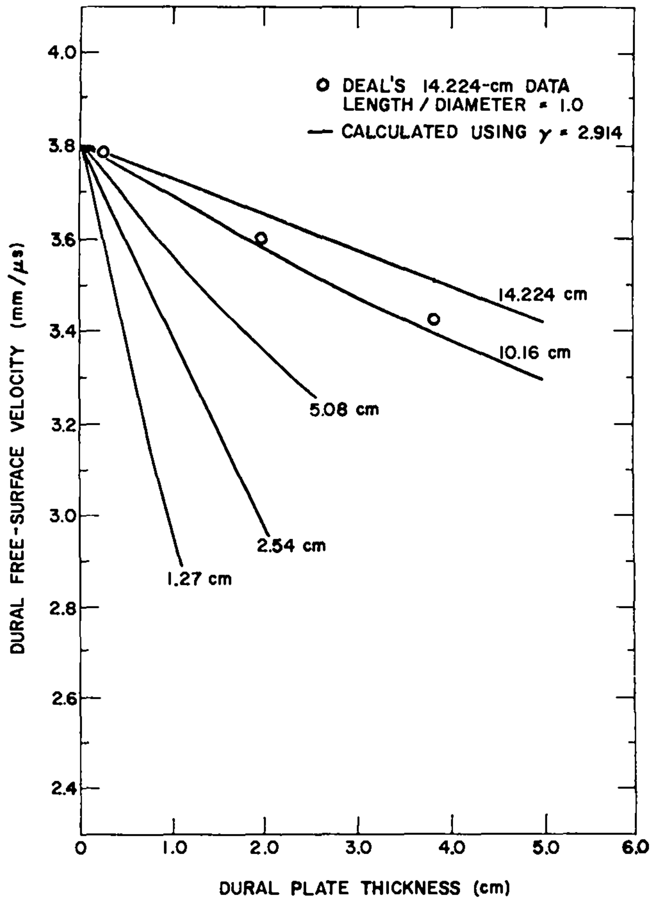


Fig. 6. Deal's experimental 9404 data for 14.224 cm of run with a two-dimensional system whose length/diameter was 1.0 are shown. The calculated results obtained for a constant gamma (2.914) Taylor wave are shown for 1.27, 2.54, 5.08, 10.16, and 14.224 cm of run. These results scale as Dural vs HE thickness, but each thickness is shown for comparison with Fig. 5.

build-up curve shown in Fig. 1 so that the curve intersects the pressure axis at whatever the initiating pressure in the explosive is for the particular driving system. Thus, if the explosive is driven with a flying plate that delivers 400 kbar to 9404, the build-up curve will be flat and no build-up will occur. If the initial pressure is greater than the infinite-medium effective C-J pressure, a decay occurs until the infinite-medium effective C-J pressure is achieved. The build-up curve shown in Fig. 1 does not address the problem of strongly overdriven detonations.

The experimental free-surface velocities for Dural include an effect of the elastic component of the rarefaction. Because this effect is nonscaling if the explosive is nonscaling, we must understand its effect on Craig's explosive build-up data. One is not certain of the yield strength of aluminum at 300-400 kbar, but a yield of 5.5 kbar successfully reproduces the Stanford Research Institute data at 330 kbar[10] and the data of Isbell et al.[11] at 250 kbar. Calculations were performed for the 9404-aluminum systems tested by Craig, using a 5.5-kbar yield and the method described in Ref. 10. The largest effect of the elastic component was to decrease the free-surface velocity by 0.01 cm/μs for the 1.27-cm-thick 9404 and 1.27-cm-thick aluminum system. Thinner aluminum plates and longer explosive distances of run resulted in correspondingly smaller effects as shown in Fig. 7. The elastic

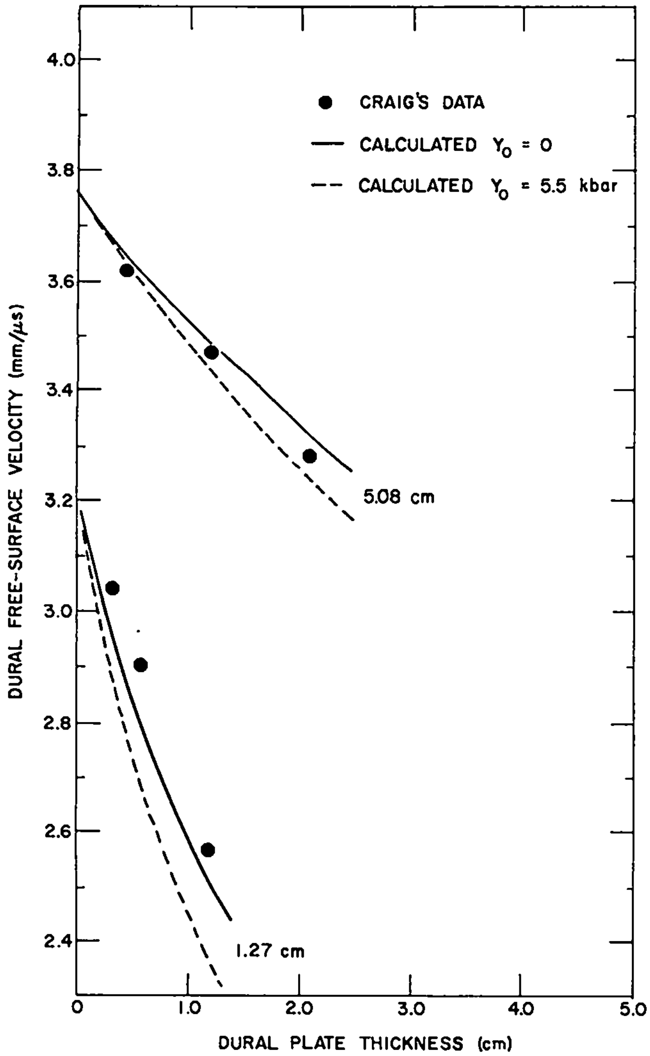


Fig. 7. Dural free-surface velocities vs Dural plate thickness for 1.27 and 5.08 cm of 9404. The calculated results for gamma of 3.77 and 2.9536 are shown for a yield of zero (as in Fig. 5) and for a 5.5-kbar yield in aluminum.

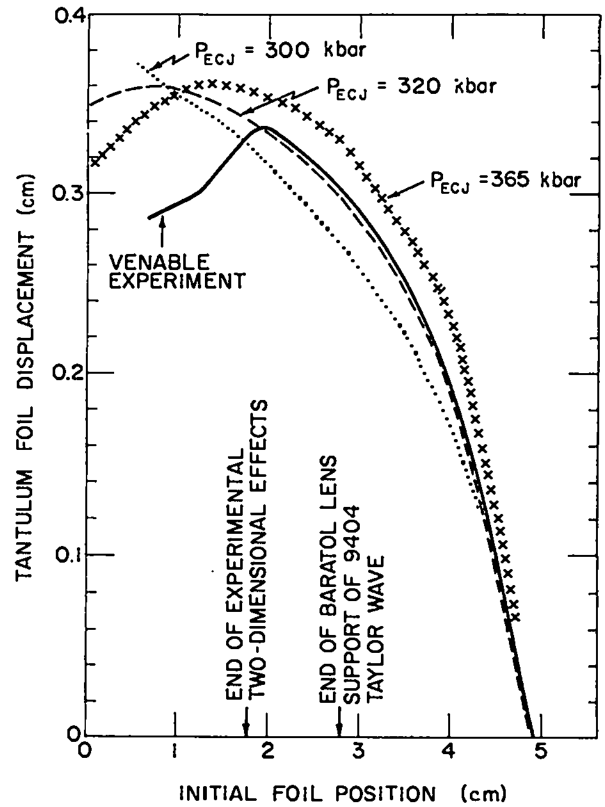


Fig. 8. Experimental tantalum foil displacements in 4.985 cm of 9404 with 0.00127-cm-thick foils embedded every 0.638 cm. The calculated displacements with effective C-J pressures of 365, 320, and 300 kbar are also shown.

effect was small compared with the build-up effect and for most of Craig's data, smaller than the experimental error.

Venable,[12] using techniques similar to those described in Ref. 13 and the PHERMEX radiographic facility, determined the behavior of a P-081 Baratol lens initiating 10.16 cm of 9404 with 0.00127-cm-thick tantalum foils embedded every 0.638 cm. The radiograph was taken after the detonation ran 4.985 cm. The effective C-J pressure for a P-081 Baratol lens initiating 5 cm of 9404 is ~365 kbar. The tantalum foils are expected to interrupt the build-up process, and the effective C-J pressure for 9404 with tantalum foils would be less than 365 kbar (the pressure with no tantalum foils) but greater than 300 kbar (the effective C-J pressure for 0.638 cm of 9404 initiated inside a 0.1-cm-thick tuballoy plate driven by 9404).

The experimental foil displacement as a function of the initial foil position is shown in Fig. 8. Also shown is the calculated displacement assuming the effective C-J pressures of 365 and 300 kbar. An effective C-J pressure of 320 kbar fits the experimental data and is additional confirmation of the importance of the build-up process. Even systems with thin foils will result in interrupting the build-up behavior and markedly decrease the observed performance.

It is important to realize that an explosive's effective C-J pressure depends on the magnitude of the initiating pulse, the distance of run, and if side rarefactions can affect the flow, upon the confinement.

## V. NITROMETHANE IN PLANE GEOMETRY

Craig measured the initial free-surface velocities of Dural plates driven by plane wave nitromethane detonations. The experimental geometries were

| Lens | TNT (cm) | Teflon (cm) | Nitromethane (20.32-cm-diam) (cm) | Plates |
|---|---|---|---|---|
| P-040 | 1.27 | 0.01524 | 2.54 | Dural |
| P-081 | 2.54 | 0.01524 | 5.08 | Dural |

These systems result in nitromethane detonation waves that are initially slightly overdriven and then decay to the infinite-medium effective C-J pressure. Although the experiments seem to scale, the 5.08-cm thickness deviates from the 2.54-cm thickness by about 1.5% at the largest scaled (Dural/nitromethane) thickness. This is larger than the experimental error (0.5%) and is probably a result of overdrive or two-dimensional effects.

Figure 9 shows the experimental data and the calculated velocities as a function of scaled Dural thicknesses for a yield of 0 and 5.5 kbar. In contrast to the underdriven 9404 data, the nitromethane data scale and do not exhibit build-up. Because the initiation of a homogeneous explosive begins in the previously shocked but undetonated explosive and proceeds through the compressed explosive at a velocity and pressure greater than the infinite-medium velocity and effective C-J pressure, the initiation of a homogeneous explosive results in an overdriven detonation that then decays toward the infinite-medium effective C-J pressure. Also, because the initiation of homogeneous explosives results in overdriven detonations in the practical case, they will not exhibit build-up. The nitromethane experimental data seem to scale and to be adequately described by a steady-state model. Although one might wish to conclude that other overdriven detonations will decay to a steady-state detonation, it is just as possible that they will decay to a flow that continues to be time dependent (oscillates), perhaps requiring greater experimental resolution to detect.

## VI. BUILD-UP IN PLANE GEOMETRY FOR TNT AND COMPOSITION B

Since the initial discovery of build-up in 9404, additional studies were made by Craig for TNT and by

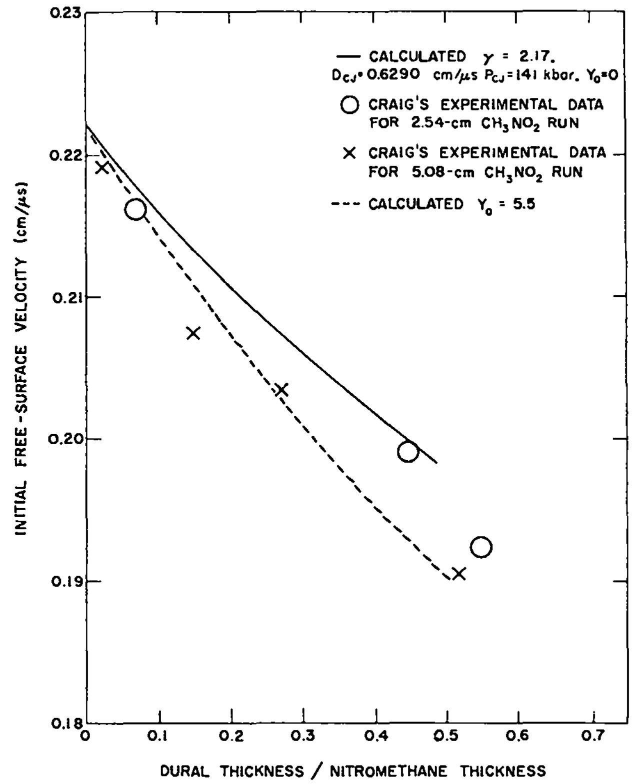


Fig. 9. Dural free-surface velocities vs the scaled Dural/nitromethane thickness for 2.54 and 5.08 cm of nitromethane. The calculated curves use the experimental infinite-medium velocity of 0.629 cm/μs, effective C-J pressure of 141 kbar, gamma of 2.17 and Dural yields of 0 and 5.5 kbar.

Davis for Composition B. Figure 10 shows that these explosives also exhibit a change in the effective detonation pressure as a function of distance of run and also a detonation velocity that remains essentially constant within the experimental measurement error. A curve is also shown for self-overdriven nitromethane for comparison with the other explosives that are underdriven by the Baratol plane wave initiation. The infinite-medium C-J pressures are shown on the right-hand side of the figure. The build-up behavior is apparently different for the various explosives, with a lesser difference between 9404 and Composition B as distances of run decrease. It seems possible that explosive build-up curves could cross and that the ordering of the performance characteristics of explosives could change, depending upon the distance of run and perhaps also on the initiating system. It is possible that some explosives may not exhibit appreciable amounts of build-up. PETN is a likely candidate for minimal build-up behavior.

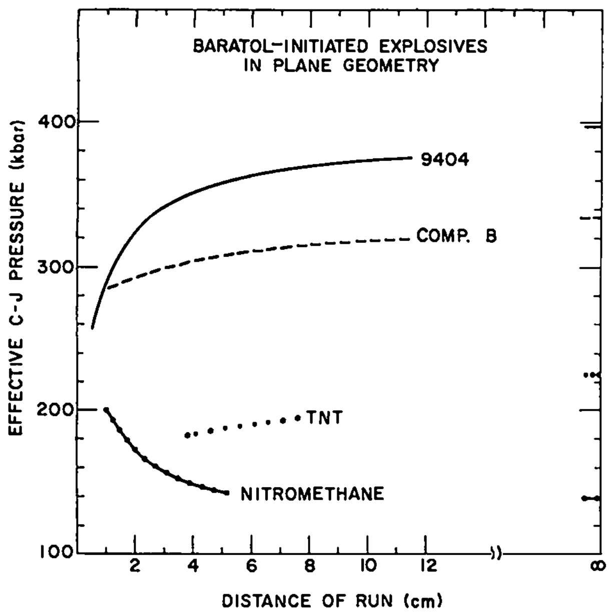


Fig. 10. Experimental effective C-J pressures of 9404, Composition B, TNT, and nitromethane initiated by a plane wave Baratol lens vs distance of run. The infinite-medium C-J pressures are shown on the right-hand side of the figure for each explosive. The nitromethane is self-overdriven and the other explosives are underdriven.

These results give quantitative significance to previous discussions[14] of the impossibility in obtaining complete agreement with experimental data for any equation of state treatment that assumes the detonations are steady-state. With the observed large effects of build-up, it is remarkable that calculations that assume steady state, such as BKW,[4] do as well as they do in reproducing the observed ordering of explosive performance. It does not seem to be profitable to attempt to make extensive studies of the equation of state of detonation products and to ignore the nonsteady-state behavior that accounts for most of the observed difference between theory and experimental performance. As stated in Ref. 14, "This complicated time-dependent behavior will have to be included into the calculation of performance of an explosive. The assumptions of chemical equilibrium will have to be dropped and detailed chemical kinetics and the time-dependent deposition of solid carbon will have to be more realistically described."

## VII. DISCUSSION OF PLANE GEOMETRY DETONATION BUILD-UP

If one investigates the experimental data for explosive systems with length-to-diameter ratios of one-half or greater, he finds that the Taylor wave is much steeper than predicted by our build-up model. Although we have attributed this to two-dimensional effects, Bdzil and Davis[9] rejected that hypothesis and developed multiple reaction zone models to describe all the data for length-to-diameter ratios up to 1.0, assuming that the experimental data are not significantly affected by the two-dimensional effects. They have been successful in reproducing the experimental data. Their excellent work provides us with another build-up model that is potentially more general and useful than the one described in this report. It remains to be proved that all the experimental data can be considered as a single set of data, regardless of the length-to-diameter ratio, over the ranges they have used. We believe that their models or some variation thereof will be very useful for engineering applications.

Even after 10 yr of effort, we have only begun to determine the actual nonsteady-state behavior of detonations, and our modeling of this process can only be classified as numerical engineering. One of the most unexpected and puzzling results of the experimental studies of recent years has been the observed constancy of the detonation velocity of an explosive and the associated large variation of the effective C-J pressures and Taylor waves. The observed lack of appreciable curvature at the front of unconfined and confined explosive charges[5] is further evidence that the detonation velocity cannot be related to the other state parameters in any simple manner.

The results of this report suggest that a rich harvest of experimental detonation performance information is possible in the future. We need to know what really happens to the build-up curves if the initiating pressures are increased or if the geometry is obviously two-dimensional. The build-up curves for other explosives with significantly different oxygen balance such as PETN would be most useful. We need to determine if the experimental build-up curves change with variations in physical properties, such as particle size and density. Without such a bank of experimental information to suggest what physical or chemical parameters should be considered, the theoretical study of build-up is nearly boundless and has little chance of addressing the problem realistically.

## VIII. DETONATIONS IN DIVERGING GEOMETRY

A theoretical treatment of a spherically expanding detonation wave does not exist. The Taylor self-similar solution for divergent detonations has been widely used for lack of a better treatment; however, Courant and Friedrichs[15] show that it is incorrect. The Taylor self-similar solution does not permit the pressure at the end of the reaction zone to change with the divergence of the flow.

Mader[3] reported the results of studies on the time-dependent reaction zones of an ideal gas, nitromethane and liquid TNT, using one-dimensional numerical hydrodynamics with the Arrhenius rate law. A similar study was made of the reaction zone in spherically diverging geometry. We have studied the reaction zone for nitromethane that was sufficiently overdriven to be stable in the plane case and for an ideal gas that was stable in the plane case at C-J velocity. Figures 11 and 12 show that the detonation process is completely dependent upon the rarefaction process following it. The pressure at the front and back of the reaction zone quickly drops below the plane wave C-J values.

We cannot follow the calculation with a resolved reaction zone for a long distance because of the limited capacity of our computers. We have performed one-dimensional numerical hydrodynamic calculations using Arrhenius kinetics and unresolved reaction zones. The important features of the flow do not depend upon the mesh size or detailed kinetics. Similar results can be obtained using C-J volume burn. For an overdriven detonation, the pressure decreases until it is considerably less than the effective C-J value and then slowly increases toward the effective C-J value. For an underdriven detonation, the pressure slowly increases toward the effective C-J value.

Craig determined the free-surface velocity of Dural plates in contact with 1.27-, 5.08-, and 7.62-cm-radius spheres, or effective spheres, of 9404 initiated by detonators varying in size from a "point"

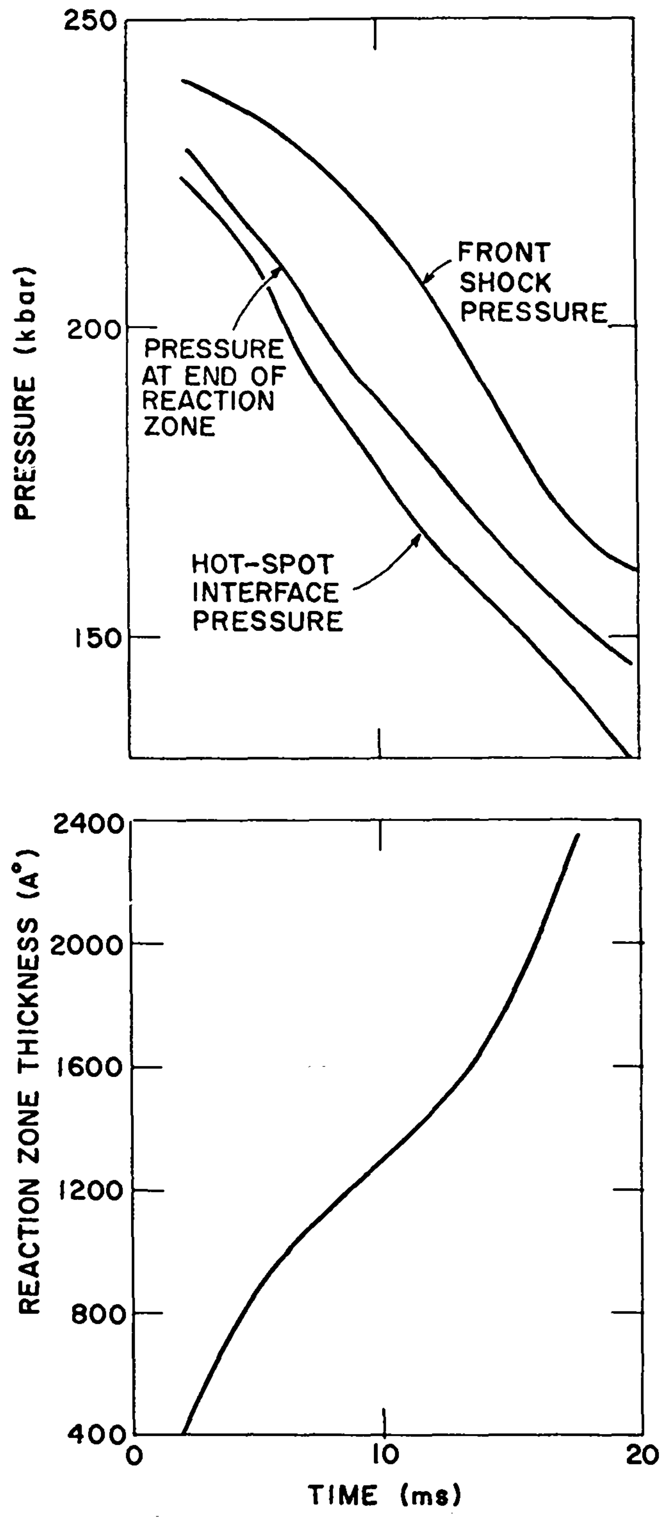


Fig. 11. Pressure and reaction zone thickness vs time for a 2.5-μm-radius hot spot driving a spherically divergent detonation in nitromethane. The calculation was performed using 100-Å mesh.

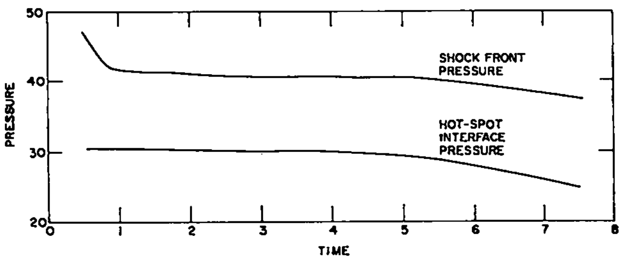


Fig. 12. Pressure vs time for a hot spot driving a spherically divergent detonation in an ideal gas described by $E^* = 10$, $f = 1.0$, $P_{W=1} = 42.2$, and $P_{W=0} = 21.5$ where $f = (D/D_{CJ})^2$, $P = P/P_o$.

of 0.1-mm radius of high-density PETN to an effective sphere of 0.76-cm radius which had low-density PETN (1.0 g/cm$^3$) for the inner 0.2 cm and high-density PETN (1.6 g/cm$^3$) for the outer 0.56 cm. The center of the 9404 detonation wave was observed to be within 0.01 cm of the center of the detonator. This is because the high-density PETN produces pressure profiles that are similar to 9404 at short distances of run.

Craig's experimental data are shown in Fig. 13. Although one might wish to conclude that the data scale, this is not the case, because the smaller radius spheres generally give lower velocities at the same scaled thickness. It is important to realize that although scaling is necessary for a Taylor self-similar model, it is not sufficient to show that the Taylor model is correct. The model used below almost scales but is not Taylor self-similar.

Calculations were performed for 1.27-, 5.08-, 7.62-, and 10.16-cm-radius spheres of 9404 and detonator, with the detonator described by a 0.2-cm-radius PETN hot spot, which initiated the surrounding 0.56-cm-thick layer of high-density PETN. The BKW or gamma-law equation of state for 9404 with an effective C-J pressure of 365 kbar and a gamma of 2.914 yielded the lower dashed curve shown in Fig. 13 for a 10.16-cm-radius sphere. The free-surface velocity of the 1.27-cm-radius sphere was ~1% less than that of the 10.16-cm-thick sphere at the same scaled thickness.

The calculated peak detonation pressure in the 9404 as a function of radius is shown in Fig. 14. For a 10-cm-radius sphere, the calculation using Arrhenius burn and BKW equation of state results in a detonation velocity of 0.8868 cm/μs and peak

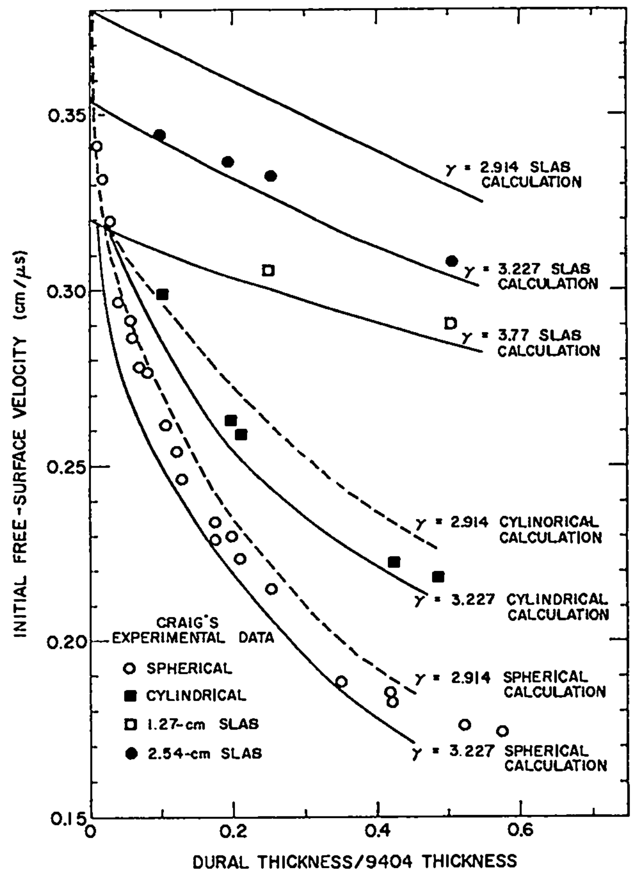


Fig. 13. Initial free-surface velocities vs scaled Dural/9404 thickness for plane, cylindrically, and spherically diverging 9404 detonations. Calculated results are shown for gammas of 2.914 (identical to results obtained using the BKW equation of state) and for gamma of 3.227 (the maximum gamma expected from build-up).

detonation pressure of 312 kbar, compared with the BKW plane wave value of 0.8880 cm/μs and effective C-J pressure of 365 kbar; thus one can apparently have differences of 53 kbar in pressure and only 12 m/s in velocity between plane and spherically diverging geometry. The experimental detonation velocities for these systems are within 100 m/s of the plane wave values.

The experimental values shown in Fig. 13 lie below the calculated curve using 365 kbar for the effective C-J pressure and gamma of 2.914. The 1.27-cm-radius values were generally below the 7.62-cm-radius points at the same scaled thickness. To obtain the maximum expected value of the build-up, we shifted the 9404 build-up curve to give the PETN effective C-J pressure of 300 kbar to the 9404 at zero

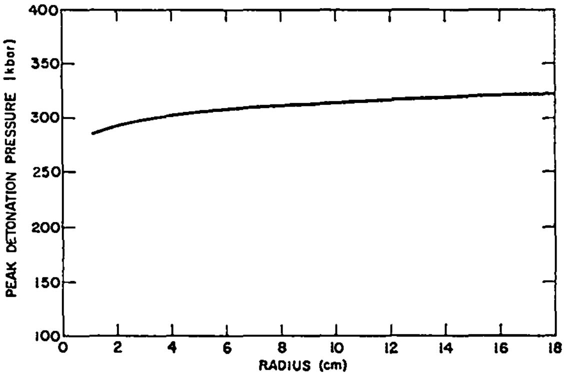


Fig. 14. Calculated peak detonation pressures of 9404 in spherically diverging geometry using a high-density PETN detonator vs detonation wave front radius.

thickness. This gives us an effective C-J pressure of 338 kbar and a gamma of 3.227 for the expected build-up equation of state of 9404 initiated with high-density PETN at the minimum (1.27 cm) distance of run studied experimentally. The bottom line in Fig. 13 shows the spherically diverging calculation with the maximum amount of build-up that can be reasonably expected. This curve is just below the experimental 1.27-cm-radius values.

Craig also determined the free-surface velocity of Dural plates in contact with 1.27-, 2.54-, and 5.08-cm-radius cylinders, or effective cylinders, of 9404 initiated with line generators of high-density PETN. Figure 13 shows the experimental and calculated results for 9404 cylinders with a gamma of 2.914 and for the maximum amount of build-up gamma of 3.227. Also shown are parts of the plane results described in Sec. IV. The build-up effect decreases with increasing divergence of the flow. The build-up effect is also small because the initiating pressures in diverging geometry are high.

Although the above agreement between the experimental data and calculations in diverging geometry is impressive, it does not suffice to show that the flow is not self-similar. It might be possible that an equation of state could be devised with a sufficiently steep isentrope to compensate for keeping the pressure at the infinite-medium effective C-J pressure as assumed in the Taylor self-similar solution. What is needed is a direct measurement of the Taylor wave pressure or density behind plane and spherically diverging detonation waves in an explosive. If the experimentally observed Taylor waves for the two systems do not give the same maximum density and pressure values, the flow is not Taylor self-similar.

Venable[12] took PHERMEX radiographs of the detonation wave of Composition B-3, using embedded tantalum foils, to determine the particle velocity and density throughout the Taylor wave in plane and spherically diverging geometry. Using a gamma-law or BKW equation of state, one obtains excellent agreement between the calculated and experimental Taylor wave densities for the front quarter of the wave as shown in Fig. 15. The experimental slab effective C-J density is 2.4 ± 0.05 g/cm$^3$ and the experimental diverging peak density is 2.2 ± 0.05 g/cm$^3$. This is conclusive evidence that the Taylor self-similar solution is incorrect and that the calculated flow in diverging geometry is adequately reproducing the actual flow.

Another diverging system, studied by Hantel and Davis,[16] for which experimental data are available is a 11.4-cm-diam, 1.69-g/cm$^3$ 9205 sphere detonated from the center by a 0.635-cm-diam spherical detonator surrounded by 13 cm of water. The BKW

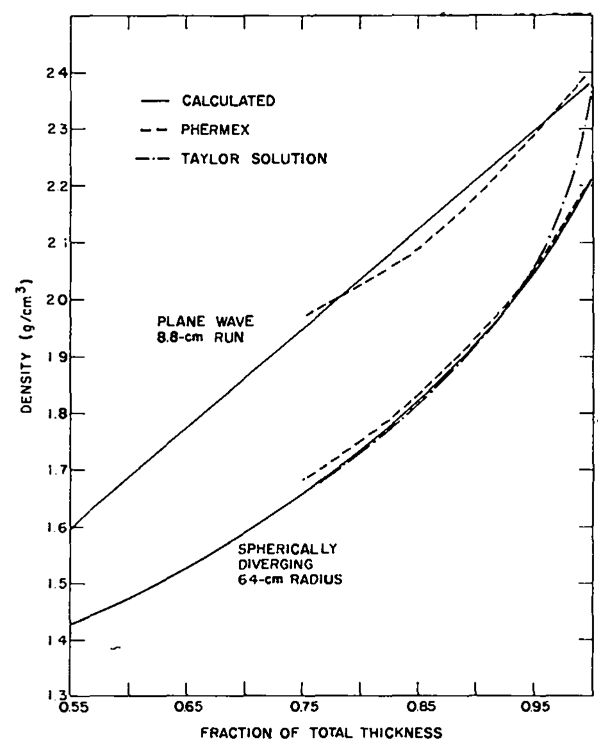


Fig. 15. Calculated and PHERMEX Taylor wave densities of 1.73 g/cm$^3$ Composition B-3 explosive.

effective C-J pressure for 9205 is 280 kbar and the calculated peak detonation pressure at the outside of the 9205 is 230 kbar. The calculated and experimental positions of the shock front as a function of time are shown in Ref. 17. They agree to within the measurement errors of the experiments.

The one-dimensional flow of spherically and cylindrically diverging detonation waves may be closely approximated numerically if the flow is not forced to be Taylor self-similar. The build-up effect in diverging geometry is masked by the larger divergence effect and higher pressure initiation systems.

## IX. DETONATIONS IN CONVERGING GEOMETRY

Converging detonations present no special numerical difficulties. One can obtain similar results for converging detonations using the Arrhenius rate law, the C-J volume burn, or the sharp-shock method, as in RICSHAW or SIN, of burning the explosive. Figure 16 shows the calculated peak detonation pressure as a function of scaled radius for spheres and cylinders of 9404 and nitromethane using either the BKW equation of state or the gamma-law equation of state with the same effective C-J pressure of 365 kbar for 9404 and the BKW equation of state for nitromethane. Figure 17 shows the detonation velocity as a function of scaled radius for a sphere of 9404. If build-up did not occur, the above results would describe the convergence effect for any size of explosive sphere, because the results scale. However, because there is build-up, one must start with different effective C-J pressures, depending upon the initial radius of the sphere and the magnitude of the initiating pulse. The results in Fig. 16 are about correct for a 10-cm-radius sphere of 9404.

As discussed in Sec. III, one requirement for using a programmed burn is a description of the change in detonation velocity with convergence. With Fig. 17 it is possible to describe the velocity for 9404 as a function of convergence for one equation of state. In our search for a more general description, we performed converging detonation calculations for 9404, Composition B, and nitromethane using different effective C-J pressures and both the SIN and RICSHAW computer codes. We found, as shown in Fig.

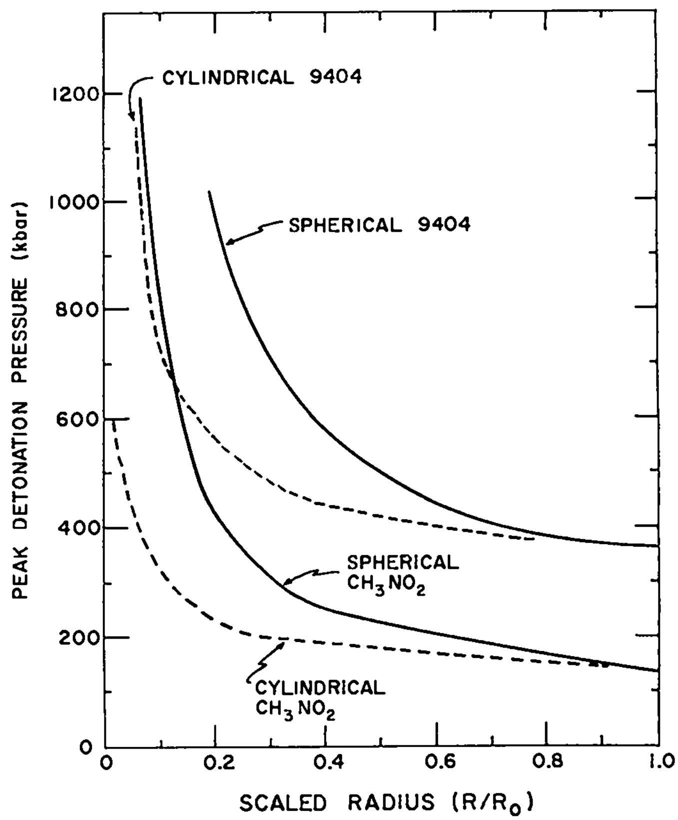


Fig. 16. Calculated peak detonation pressures vs scaled radius for spherically and cylindrically converging detonations of 9404 and nitromethane.

18, that the results could be scaled as the peak detonation pressure divided by the effective C-J pressure as a function of the scaled radius. Figure 19 shows that one can obtain a similar scaled plot for the detonation velocity.

As a good first approximation, the detonation velocity, D, can be described as a function of the detonation front radius divided by the initial radius, $R/R_o$, in spherical geometry by

$$\frac{D}{D_{CJ}} = 0.22049 \left(\frac{0.2}{R/R_o}\right)^{1.65} + 0.9845 \quad ,$$

$$\text{for } 1.0 < \frac{R}{R_o} > 0.25 \quad ,$$

and in cylindrical geometry by

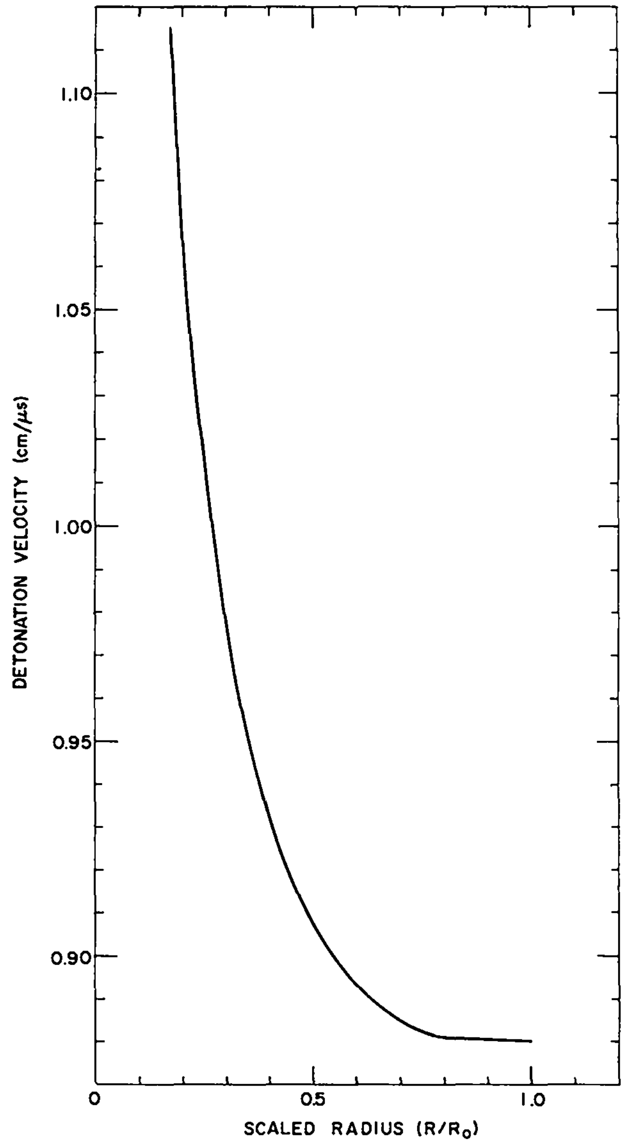


Fig. 17. Calculated detonation velocities vs scaled radius for a spherically converging 9404 detonation.

$$\frac{D}{D_{CJ}} = 0.1255 \left(\frac{0.1}{R/R_o}\right) + 0.9875 \quad ,$$

$$\text{for } 1.0 < \frac{R}{R_o} > 0.15 \quad .$$

These equations permit converging detonation calculations using the programmed velocity burn down to $R/R_o$ of at least 0.5. They must be used with care because they are approximate, and other equations of state could give different convergence effects.

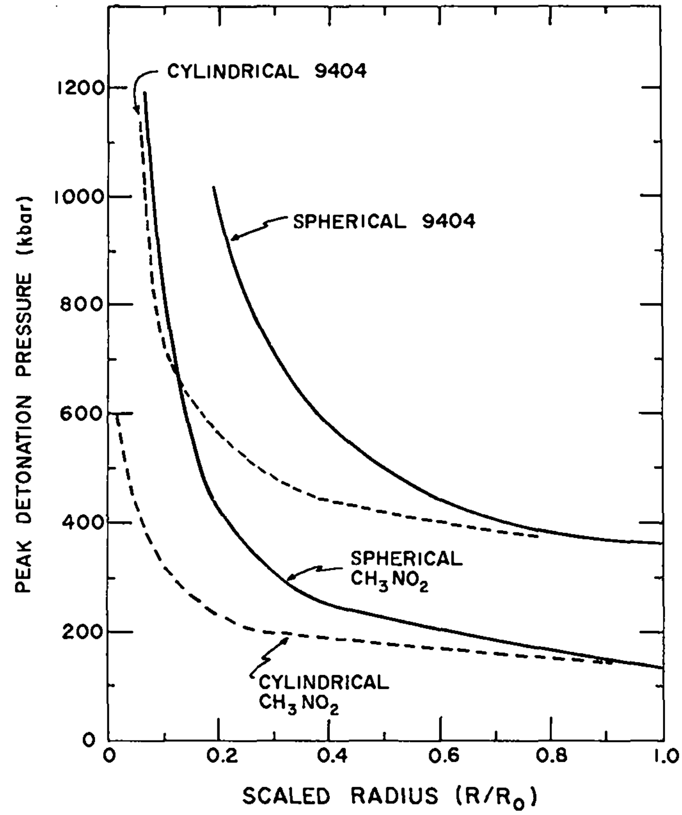


Fig. 18. Scaled peak detonation pressures vs scaled radius for spherically and cylindrically converging detonations of 9404, nitromethane, and Composition B.

Experimental evidence that the calculated converging detonation wave profiles are realistic has been collected by Morales and Venable[18] using the PHERMEX facility. They detonated a 9404 sphere 12.319 cm in outside radius and studied the shock wave formed when the converging detonation wave interacted with a 3.048-cm-radius aluminum sphere. Embedded foils permitted the determination of the density profile before and after the shock wave had converged at the center of the sphere. The explosive was described with an effective plane C-J pressure of 365 kbar. The peak detonation pressure upon arrival of the detonation front at the surface of the aluminum sphere was 820 kbar. The calculated timing of the arrival of the detonation front agreed with the experimental observations. The 1100 aluminum had an initial density of 2.710 g/cm$^3$ and the equation of state used was $U_s = 0.5222 + 1.428\ U_p$ with a gamma of 1.7. Above 5 Mbar, the Barnes[19]

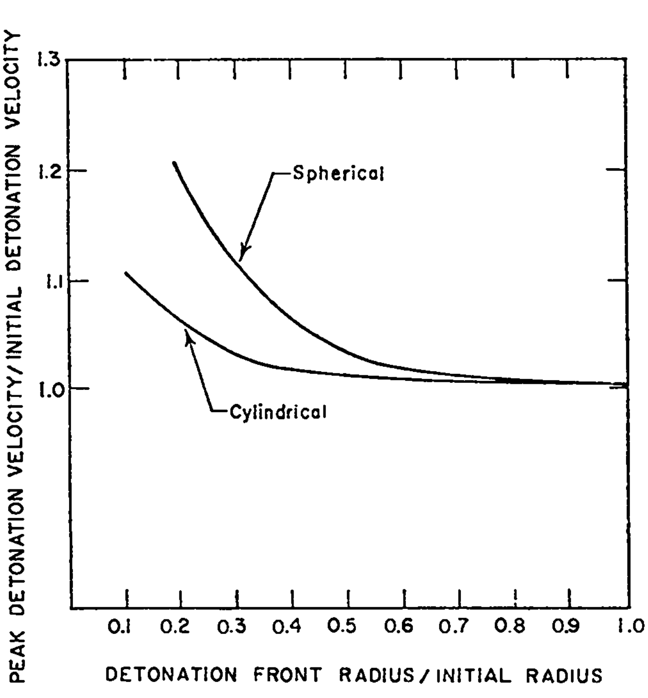


Fig. 19. Scaled detonation velocities vs scaled radius for the same explosives as in Fig. 18.

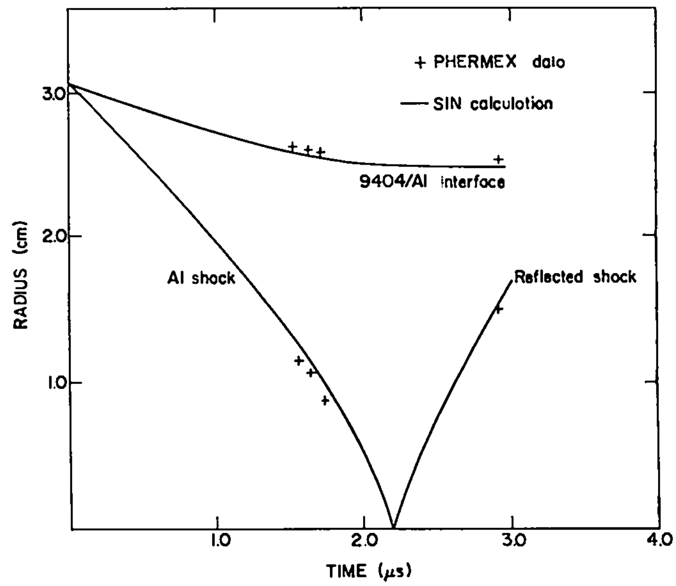


Fig. 20. Radius vs time profiles of the shock waves and interfaces inside a 3.048-cm-radius sphere of aluminum shocked by a surrounding sphere of 9.271-cm-thick 9404. PHERMEX radiographic data are shown at four different times.

equation of state was used. Figure 20 shows the calculated and experimental positions of the shock waves and interface, and Fig. 21 shows the foil position through the shock wave in aluminum at 1.63 μs after the shock arrived at the explosive-aluminum interface. Such good agreement with the experimental results indicates that the calculated convergent detonation profile is realistic.

## X. CONCLUSIONS

The detonation process for 9404 in plane, diverging, and converging geometry is not steady state. The 9404 infinite-medium effective C-J pressure of 400 kbar is achieved only after a great distance of run, using initiating systems that initially shock the explosive to < 300 kbar. The build-up process of the effective C-J pressure of 9404 was reproduced using an empirical build-up model calibrated with experimental data for one-dimensional systems in plane, diverging, and converging geometry. Similar build-up behavior was observed for Composition B and TNT.

The observed small changes of detonation velocity in plane and diverging geometry that are associated with large changes in the effective C-J pressure and the Taylor waves suggest that our usual steady-state detonation models are unrealistic. The physical and/or chemical processes that are rate-

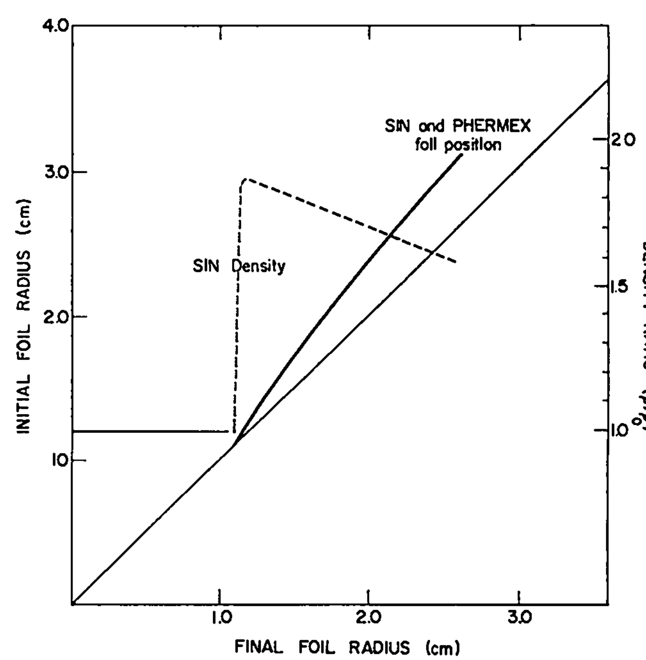


Fig. 21. Initial and final foil radii and the shock wave density for the system described in Fig. 20 at 1.63 μs after detonation wave arrived at the surface of aluminum sphere.

determining in the detonation process are unknown. Extensive experimental studies will be required to determine the nature of these processes.

The practical consequences of the nonsteady-state behavior of explosives have been elucidated. Our previous attempts to describe an explosive with a single effective C-J pressure, regardless of the distance of run or the initiating systems, were as certain of failure as if we had used a single C-J pressure and velocity to describe all explosives. We look forward to increased understanding of the detonation process that may occur as we abandon the mental strait jacket of steady-state theory.

ACKNOWLEDGMENTS

We wish to express our appreciation to J. Bdzil, W. C. Davis, W. Fickett, D. Venable, L. C. Smith, G. N. White, Jr., H. Hoyt, R. Orr, R. Morales, W. Rivard, M. Berger, G. Wall, G. Brotbeck, B. Mudd, R. Swanson, C. Forest, J. R. Travis, A. W. Campbell, and J. Barnes for their contributions and helpful discussions. The theoretical studies were performed in the Theoretical Division of the Los Alamos Scientific Laboratory.

REFERENCES

1. B. G. Craig, Los Alamos Scientific Laboratory, unpublished data, 1965.

2. W. C. Davis, B. G. Craig, and J. B. Ramsay, "Failure of the Chapman-Jouguet Theory for Liquid and Solid Explosives," Phys. Fluids 8, 2169 (1965).

3. Charles L. Mader, "One- and Two-Dimensional Flow Calculations of the Reaction Zones of Ideal Gas, Nitromethane, and Liquid TNT Detonations," in Twelfth Int. Symp. on Combustion, (The Williams and Wilkins Company, Baltimore, MD, 1968), p. 701.

4. Charles L. Mader, "Detonation Properties of Condensed Explosives Computed Using the Becker-Kistiakowsky-Wilson Equation of State," Los Alamos Scientific Laboratory report LA-2900 (February 1963).

5. Charles L. Mader, "Detonation Induced Two-Dimensional Flows," Acta Astronaut. 1, 373 (1974).

6. Charles L. Mader, "An Empirical Model of Heterogeneous Shock Initiation of 9404," Los Alamos Scientific Laboratory report LA-4475 (October 1970).

7. Charles L. Mader and William R. Gage, "FORTRAN SIN. A One-Dimensional Hydrodynamic Code for Problems which Include Chemical Reactions, Elastic-Plastic Flow, Spalling, and Phase Transitions," Los Alamos Scientific Laboratory report LA-3720 (September 1967).

8. B. D. Lambourn and N. E. Hoskins," The Computation of General Problems in One-Dimensional Unsteady Flow by the Method of Characteristics," Fifth Int. Symp. on Detonation, Office of Naval Research report DR-163 (1970); also Methods Comput. Phys. 3, 265 (1964).

9. J. B. Bdzil and W. C. Davis, "Time-Dependent Detonations," Los Alamos Scientific Laboratory report, in preparation (1975).

10. Charles L. Mader, "One-Dimensional Elastic-Plastic Calculations for Aluminum," Los Alamos Scientific Laboratory report LA-3678 (June 1967).

11. W. M. Isbell, F. H. Shipmann, and A. H. Jones, "Use of a Light Gas Gun in Studying Material Behavior at Megabar Pressures," in Behavior of Dense Media Under High Dynamic Pressures, (Gordon and Breach Science Publishers, New York, 1968), p. 179.

12. Douglas Venable, Los Alamos Scientific Laboratory, private communication (1968).

13. W. C. Rivard, D. Venable, W. Fickett, and W. C. Davis, "Flash X-Ray Observations of Marked Mass Points in Explosive Products," Fifth Int. Symp. on Detonation, Office of Naval Research report DR-163 (1970).

14. Charles L. Mader, "Numerical Calculations of Explosive Phenomena," in Computers and Their Role in the Physical Sciences, (Gordon and Breach Science Publishers, New York, 1970), p. 385.

15. R. Courant and K. O. Friedrichs, Supersonic Flow and Shock Waves, (Interscience Publishers, New York, 1948), p. 430.

16. L. W. Hantel and W. C. Davis, "Spherical Explosions in Water," Fifth Int. Symp. on Detonation, Office of Naval Research report DR-163 (1970).

17. Charles L. Mader, "Compressible Numerical Calculations of Underwater Detonations," Los Alamos Scientific Laboratory report LA-4594 (March 1971).

18. R. Morales and D. Venable, Los Alamos Scientific Laboratory, private communication (1974).

19. John F. Barnes, "Statistical Atom Theory and the Equation of State of Solids," Phys. Rev. 153, 269 (1967).

☆US GOVERNMENT PRINTING OFFICE 1975—677-180/46